Applied Catalysis B: Environmental 96 (2010) 496–507

Contents lists available at ScienceDirect

Applied Catalysis B: Environmental

journal homepage: www.elsevier.com/locate/apcatb

$CoMo/Al_2O_3$-SiO_2 catalysts prepared by co-equilibrium deposition filtration: Characterization and catalytic behavior for the hydrodesulphurization of thiophene

John Vakros[a,*], Alexis Lycourghiotis[a], G.A. Voyiatzis[b], A. Siokou[b], Christos Kordulis[a,b]

[a] Department of Chemistry, University of Patras, GR 265 00, Rion-Patras, Greece
[b] Institute of Chemical Engineering & High Temperature Chemical Processes (FORTH / ICE-HT), P.O. Box 1414, GR-265 00, Patras, Greece

ARTICLE INFO

Article history:
Received 16 December 2009
Received in revised form 3 March 2010
Accepted 5 March 2010
Available online 12 March 2010

Keywords:
CoMo catalysts
Hydrotreatment
Silicoaluminas
Catalyst preparation
EDF
Mo-deposition
DRS
LRS
TPR
HDS

ABSTRACT

Four CoMo catalysts supported on Al_2O_3-SiO_2 mixed materials of varying SiO_2 content (1.5, 10, 20 and 30% SiO_2 w/w) were prepared following the co-EDF methodology. The catalysts were characterized using various techniques (BET, potentiometric mass titrations, XRD, DRS, XPS, LRS, TPR, TPD of ammonia and NO chemisorption). Two additional catalysts were prepared and characterized on two mixed supports, which contain 1.5 and 20% SiO_2 w/w, following the conventional impregnation procedure. The hydrodesulphurization (HDS) activities of the catalysts studied were determined using thiophene as a probe molecule.

The co-EDF catalysts were proved to be more active than the corresponding ones prepared following the conventional impregnation procedure. This was attributed to the relatively high dispersion of the Mo supported phase achieved by applying co-EDF. The following activity trend was obtained over the co-EDF catalysts, 20Si > 30Si > 1.5Si > 10Si, which indicates that the activity is maximized over the catalyst prepared on a mixed support containing 20% SiO_2 w/w. This zigzag trend was explained in terms of two parameters, the ratio "tetrahedral (monomer) /octahedral (polymer) Mo species" and the amount of cobalt aluminate formed, both regulated by changing the composition of the mixed support.

1. Introduction

Hydrodesulphurization (HDS) is a key reaction for producing clean fuels. The environmental regulations relevant to sulphur specifications for transportation fuels become more and more strict. A critical issue is that a significant part of the reserves of some oil-producing countries consists of heavier fractions with a high content of contaminants. Among these contaminants sulphur is significant. The demand for lower sulphur content in fuels requires the development of more active HDS catalysts. These catalysts usually consist of supported MoS_2 on an alumina carrier promoted by cobalt or nickel [1]. The use of some additives (e.g. P, F, B) in the catalyst formulations [1–9] or the addition of some chelating compounds in the impregnation solution [10–17] are proved to be important tools for improving the HDS activity of the catalysts.

The modification of the preparation procedure is another approach. The impregnation step, the most important in the preparation sequence, is usually carried out following the conventional incipient wetness or wet impregnation techniques. In the last years we have developed an alternative impregnation methodology, *the equilibrium deposition filtration technique* (EDF) [18–20]. The application of EDF for depositing the Mo(VI) species, or both the Mo(VI) and Co(II) species, on the γ-alumina surface (co-EDF), has resulted in more active catalysts than those prepared by the conventional impregnation techniques [21–23]. More precisely, $CoMo/\gamma$-Al_2O_3 catalysts prepared by EDF were proved to be about 30–43% more active in HDS than the corresponding catalysts prepared following the conventional impregnation techniques. Moreover, these catalysts exhibited relatively low hydrogenation activity. Thus, EDF or co-EDF could be used for the preparation of very active $CoMo/\gamma$-Al_2O_3 catalysts for deep hydrodesulphurization of oil with relative low hydrogen consumption.

A third approach for improving HDS activity is by using new supports. Many studies have shown that one of the major factors affecting this activity is the interaction between the active components and the support. A large number of new materials have been developed and tested [24–31]. Among these materials the mixed Al_2O_3-SiO_2 supports are quite promising. La Parola et al. [26] studied the HDS activity and the structural properties of CoMo catalysts supported on mixed Al_2O_3-SiO_2 supports of varying alumina content (0–100%). It was found that the HDS activity depends on the Al/Si atomic ratio. The maximum activity was obtained using

* Corresponding author. Tel.: +30 2610997143; fax: +30 2610994796.
E-mail address: vakros@chemistry.upatras.gr (J. Vakros).

0926-3373/$ – see front matter © 2010 Elsevier B.V. All rights reserved.
doi:10.1016/j.apcatb.2010.03.011

a mixed Al_2O_3-SiO_2 support (66% Al_2O_3 and 34% SiO_2). The activity profile was related to the dispersion and the reducibility of the active species determined by the acidity of the support. On the mixed oxide with the aforementioned composition a good compromise was obtained between dispersion and reduction during sulphidation. Dalama and Stanislaus [27] studied the HDS activity of a series of CoMo catalysts supported on γ-alumina and a mixed Al_2O_3-SiO_2 support containing 30% SiO_2. The impregnation solution used was free or contained a chelating agent. The HDS activities of all catalysts were tested in a micro reactor using straight run gas oil as feed. The catalysts prepared using SiO_2–Al_2O_3 as support were remarkably more active than those prepared using γ-Al_2O_3. A deep hydrodesulphurization of diesel to ultra low sulphur levels (<15 ppm) was obtained over a catalyst with high Mo and Co loading developed on the Al_2O_3-SiO_2 support. CoMo HDS catalysts were recently developed using Al modified mesoporous silicas [28–31]. A good synergy between Al and Si has been found in all cases. It is important to stress that in all cases the CoMo catalysts supported on mixed Al_2O_3-SiO_2 supports or Al modified mesoporous silicas have been prepared using the conventional incipient or co-incipient wetness impregnation.

In the present work we combine the EDF methodology and the use of mixed silica-alumina supports for improving further the catalytic HDS activity of the CoMo catalysts. More precisely, we prepared a series of CoMo catalysts supported on Al_2O_3-SiO_2 mixed materials of varying SiO_2 content (1.5, 10, 20 and 30% SiO_2 w/w) *following the co-EDF methodology*. The catalysts were characterized using various techniques. The hydrodesulphurization (HDS) activities over the catalysts studied were determined using thiophene as a model molecule. For comparison, two additional catalysts were prepared and characterized on two mixed supports (1.5 and 20% SiO_2 w/w) following the conventional impregnation technique. These catalysts have been also tested using the same probe reaction.

2. Experimental

2.1. Equilibrium deposition experiments

Isotherms were obtained at 25 °C and various pHs for studying the deposition of Mo(VI) oxo-species and Co(II) aqua complexes on pure γ-alumina (Condea) and silica (Alfa Aesar). Ammonium heptamolybdate (Merck, analytical grade) and cobalt nitrate hexahydrate (Merck, analytical grade) were used for preparing the Mo(VI) and Co(II) solutions, respectively. The initial concentrations of Mo(VI) varied in the range 0–5×10^{-2} M (γ-alumina) and 0–2×10^{-2} (silica). The initial concentrations of Co(II) varied in the range 0–4×10^{-2} M for both γ-alumina and silica. The photometric determination of the Mo concentration in the impregnation solution was performed at 490 nm, before and after adsorption of the Mo(VI) oxo-species, following the catechol method described by Snell [32]. The deposited amount of Mo was calculated from the difference in the two concentration values. The Co^{2+} deposition was also determined photometrically at 560 nm by measuring the Co^{2+} concentration in the impregnating solution before and after deposition. The determination was based on the Nitroso R-salz procedure [33]. A spectrophotometer (Cary 3 Varian) was used in all cases. Details concerning the equilibrium deposition experiments have been reported elsewhere [34].

2.2. Preparation of the specimens

Four CoMo/Al_2O_3-SiO_2 co-EDF samples (denoted by 1.5Si, 10Si, 20Si and 30Si) were prepared using four Al_2O_3-SiO_2 mixed supports of varying silica content (1.5, 10, 20 and 30% SiO_2 w/w). These powdered supports were obtained from Condea. Following the co-EDF technique [22], the molybdenum(VI) oxo-species and the cobalt(II) aqua complexes were deposited onto the surface of the supports at 25 °C from a mixed Co–Mo solution (2.5×10^{-2} M Mo and 2×10^{-2} M Co). Ammonium heptamolybdate (Merck, analytical grade) and cobalt nitrate hexahydrate (Merck, analytical grade) were used for preparing the mixed solutions. The amount of the deposited Mo and Co was determined spectrophotometrically [32,33]. Following the co-EDF technique the deposition takes places during the equilibration of the suspension. The pH was kept constant at 4.9 upon equilibration. The samples were dried in air at 110 °C for 2.5 h and then air-calcined at 500 °C for 5 h. In order to compare the influence of the preparation method on the catalytic activity we prepared two additional samples, corresponding to the samples 1.5Si and 20Si, following the conventional procedure. In these samples Mo was deposited first by wet impregnation following by drying and calcination. The cobalt was then deposited by incipient wetness impregnation followed by drying and calcination. The drying and calcination conditions were those mentioned before. These conventionally prepared samples are denoted by $1.5Si_{conv}$ and $20Si_{conv}$. The samples $1.5Si_{conv}$ and $20Si_{conv}$ contain the same amount of the supported cobalt and molybdenum to the samples 1.5Si and 20Si, respectively.

2.3. Characterization of the specimens and determination of their catalytic activity

2.3.1. Specific surface area (SSA)

Specific surface area measurements have been carried out by the three-point dynamic BET method using a laboratory-constructed apparatus. Pure nitrogen and helium (Air Liquide) were used as adsorption and carrier gas, respectively. A thermal conductivity detector (VICI, Valco Instruments Co. Inc.) was used for the detection of the adsorbed amount of nitrogen at a given partial pressure.

2.3.2. Diffuse reflectance spectroscopy (DRS)

The diffuse reflectance spectra of the samples studied were recorded in the range 200–800 nm at room temperature using a UV–vis spectrophotometer (Varian Cary 3) equipped with an integration sphere. The carrier was used as a reference in all cases. The powder samples were mounted in a quartz cell which provided a sample thickness greater than 3 mm and thus guaranteed "infinite" sample thickness.

2.3.3. X-ray photoelectron spectroscopy (XPS)

The XPS analysis of the oxidic specimens was performed at room temperature in an UHV chamber (base pressure 8×10^{-10} mbar) which consists of a fast specimen entry assembly, a preparation and an analysis chamber. The residual pressure in the analysis chamber was below 10^{-8} mbar. The latter was equipped with a hemispherical electron energy analyzer (SPECS, LH10) and a twin-anode X-ray gun for XPS. The unmonochromatized Mg KR line at 1253.6 eV and a constant pass energy mode for the analyzer were used in the experiments. Pass energies of 36 and 97 eV resulted at a full width at half-maximum (fwhm) of 0.9 and 1.6 eV, respectively, for the Ag $3d_{5/2}$ peak of a reference foil. The binding energies were calculated with respect to the C1s peak (C–C, C–H) set at 285.5 eV. The normalized intensities I_{Mo3d}, I_{Co2p}, I_{Al2p}, I_{Si2p} and I_{O1s} of the corresponding XPS peaks, corrected using the sensitivity factors published by Wagner et al, [35–36] were used to determine the atomic surface composition of the catalysts studied.

2.3.4. Temperature-programmed reduction (TPR)

The TPR experiments were performed in laboratory-constructed equipment, in which the ideas of the Rogers–Amenomiya–Robertson arrangement [37] have been followed. An amount of sample, 0.1 g, was placed in a quartz reactor and the reducing gas mixture (H_2/Ar:5/95 v/v) was passed

through it for 2 h with a flow rate of 40 mL min^{-1} at room temperature. Then the temperature was increased to 1000 °C with a constant rate of 10 °C min^{-1}. Reduction leads to a decrease of the hydrogen concentration of the gas mixture, which was detected by a thermal conductivity detector (TCD). The reducing gas mixture was dried in a cold trap (−95 °C) before reaching the TCD.

2.3.5. Laser Raman spectroscopy

Raman spectra of the samples studied were excited with the 514.5 nm line of a Spectra Physics (model 163-A42) air-cooled Ar^+ laser. The spectral resolution was 3 cm^{-1}. A small-band pass interference filter was used for the laser plasma lines elimination. The excitation beam was directed to a proper modulated sample compartment of a metallurgical microscope (Olympus BHSM-BH2). The microscope was used for the delivery of the excitation laser beam on the sample and the collection of the backscattered light through a beam-splitter and the objective lens adapted to the aperture of the microscope. The focusing objective lens was a Long Working Distance (8 mm) 50–0.55 Olympus lens. The spectra were obtained with a power of 3 mW on the specimen for an integration time of 2–100 s. A viewing screen connected to the microscope offered good sample positioning, good laser beam focusing and direct surface inspection. The T-64000 (Jobin Yvon) Raman system equipped with a Spectraview-2DTM liquid N_2 cooled CCD detector was used, in the triple subtractive configuration, to filter scattered light for the Rayleigh elastic scattering removal, and to disperse and detect the Raman signal.

2.3.6. X-ray powder diffraction (XRD)

The XRD patterns of the powdered samples were recorded using an ENRAF NONIOUS FR 590 diffractometer. A Cu Kα (1.54198 A°) radiation has been used. The generator was equipped with a curved position sensitive detector CPS120 of INEL. This was operated at 45 kV and 25 mA.

2.3.7. Temperature-programmed desorption of NH_3 (TPD)

The TPD experiments were performed in laboratory-constructed equipment. An amount of sample, 0.1 g, was placed in a quartz reactor and the gas mixture (NH_3/He:5/95 v/v) was passed through it for 2 h with a flow rate of 40 mL min^{-1} at room temperature to ensure the complete adsorption of NH_3. Then the temperature was increased up to 500 °C with a constant rate of 10 °C min^{-1}. The amount of NH_3 desorpted was detected by a thermal conductivity detector (TCD).

2.3.8. NO adsorption

The dynamic method was used to study the chemisorption of nitric oxide in laboratory-constructed equipment. A pre-weighted amount of the oxide catalyst (100 mg) was introduced into the vessel which was then connected via the four-port valve in a sulphidation apparatus. The sulphidation procedure was that followed in catalytic tests. The sample was then cooled down to room temperature and transported to the nitric oxide adsorption equipment where it remained for 1 h under a stream of helium. Pulses of the adsorption mixture [NO–He (5:95 v/v)] were introduced every 3 min. The amount of nitric oxide eluted after each injection was measured until two successive pulses gave a difference less than 1%. The total uptake of nitric oxide was thus determined. The catalyst was then maintained for 1 h under a stream of pure helium and the procedure was repeated. The difference in the uptake of nitric oxide during the first and the second adsorption cycle was considered to be equal to the amount of the chemisorbed nitric oxide. Full experimental details concerning the above characterization techniques have been reported elsewhere [22,38]. The values of the point of zero charge of the mixed supports were determined using the recently developed *potentiometric mass titration technique* [39,40].

2.3.9. Determination of catalytic activity

The hydrodesulphurization (HDS) activities over the catalysts studied were determined using thiophene as a probe molecule and a continuous-flow tubular fixed-bed micro reactor operating in a differential mode at atmospheric pressure. The catalyst samples (50 mg) were presulfided in situ, with a stream of 15% (v/v) hydrogen sulfide in hydrogen, for 2 h at 400 °C. The reaction mixture was prepared by passing hydrogen through a flow evaporator filled with liquid thiophene at 0 °C. After an aging period of 15 h under the stream of the reaction mixture the rate of thiophene HDS was determined over each catalyst at various temperatures in the range 250–320 °C. Full experimental details concerning the activity tests have been reported elsewhere [41].

3. Results

3.1. Equilibrium deposition experiments on pure γ-alumina and silica

The deposition isotherms obtained for the deposition of the Mo(VI) species on pure γ-alumina and silica are illustrated in Fig. 1a and b, respectively.

The Mo deposition on γ-alumina is described by Langmuir type isotherms. Moreover, the extent of deposition increases as pH decreases. This behavior is expected. It is, moreover, in full agreement with the established deposition mechanism [42,43]. The deposition isotherms derived for silica at pH 6 show that there is not practically deposition of the Mo oxo-species, irrespectively of the Mo(VI) solution concentration. An abrupt increase, in the extent of the Mo(VI) deposition, was observed at pH 5.0 and above a concentration value equal to 0.7×10^{-3} M. This increase and the development of yellow color in the impregnation solution strongly suggest surface dissolution of the silica surface and precipitation of silicomolybdenic acid [44,45]. The aforementioned precipitation

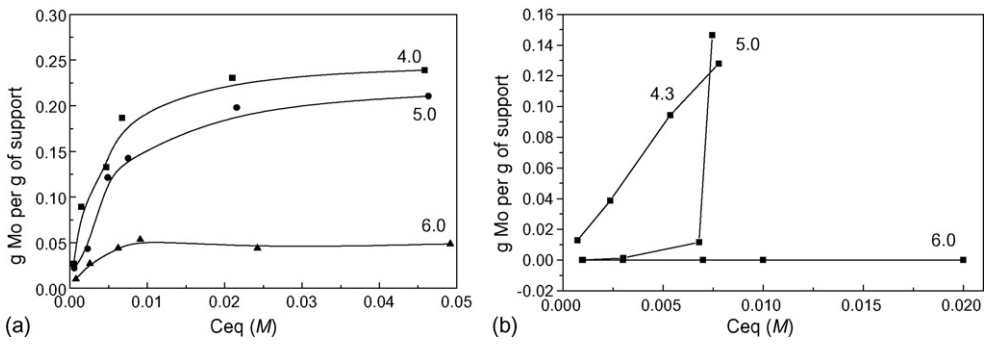

Fig. 1. Isotherms obtained at 25 °C and various pHs for the deposition of Mo(VI) oxo-species on the γ-alumina (a) and silica (b) surface. The pH values are indicated.

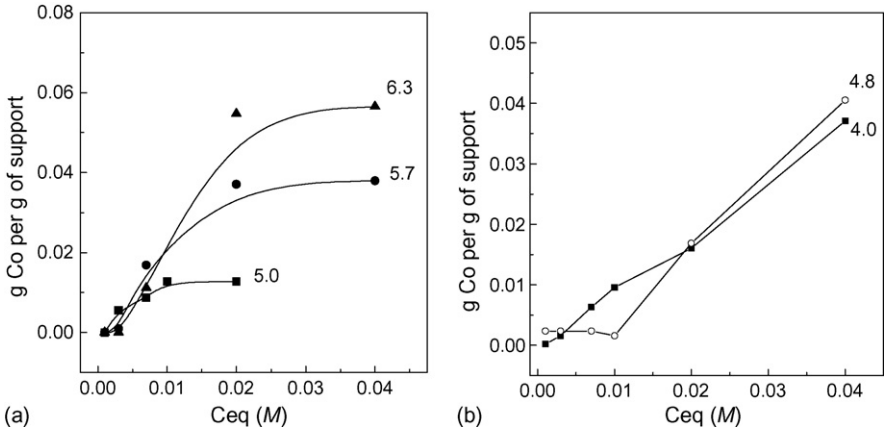

Fig. 2. Isotherms obtained at 25 °C and various pHs for the deposition of Co(II) aqua complexes on the γ-alumina (a) and silica (b) surface. The pH values are indicated.

was also observed at pH 4.3, even at lower Mo(VI) concentrations of the impregnating solution.

The deposition isotherms obtained for the deposition of the Co(II) species on pure γ-alumina and silica are illustrated in Fig. 2a and b, respectively.

The Co deposition on γ-alumina is described by Langmuir type isotherms. Moreover, the extent of deposition increases as pH increases. This behavior is also expected. Moreover, it is in full agreement with the established deposition mechanism [46–50]. The Co deposition on silica is described by linear type isotherms. This indicates that the silica surface remains unsaturated after deposition in the whole range of the solution Co(II) concentrations studied.

3.2. Loading, specific surface area and point of zero charge

Some physicochemical parameters of the supports and the catalysts prepared are illustrated in Table 1.

Let's start with the co-EDF catalysts (rows 1, 3, 4 and 6). We observe that the MoO_3 content decreases as the silica content increases. In contrast, the MoO_3 content remains practically constant with respect to the alumina component of the support. The CoO loading remains practically constant. We observe, moreover, an increase of the support surface area with the silica content in the mixed supports. In contrast, a considerable decrease in the specific surface area is observed after the deposition of the CoMo phase, drying and calcination. However, the decrease is rather small (8–15.5%) provided that the specific surface area is expressed per gram of the mixed support contained in the co-EDF catalysts (values in parenthesis). A shift of the p.z.c. value of the mixed supports with the silica content was observed from that of pure alumina (ca. 8.2) to that of pure silica (ca. 2.9). This is in agreement to the literature [51]. The picture is similar for the conventional catalysts (lines 2 and 5). However, the decrease in the specific surface area observed after the deposition of the CoMo phase, drying and calcination is more pronounced.

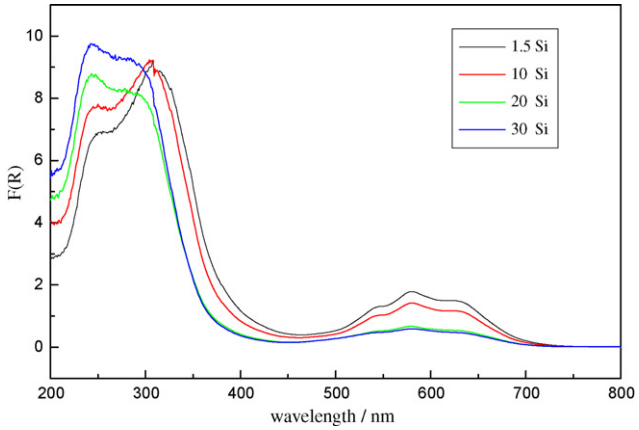

Fig. 3. Diffuse reflectance spectra recorded for the calcined co-EDF samples in the range 200–800 nm.

3.3. X-ray diffraction

Only the diffraction peaks due to the γ-alumina crystallites appear in the XRD spectra of the catalysts studied (not shown here). The magnitude of these peaks decreases with the increase of the content of the amorphous silica in the mixed support.

3.4. Diffuse reflectance spectroscopy

The DR spectra recorded in the range 200–800 nm for the co-EDF catalysts are illustrated in Fig. 3. The characteristics bands of the supported cobalt molybdena catalysts appear in these spectra. The wide absorption band below 350 nm is comprised of two peaks at 240–270 and 290–320 nm due to the molybdena tetrahedral and octahedral supported species, respectively [52–54]. The first is centered at about 265 nm whereas the second at about 305 nm. Moreover, the characteristic triplet band assigned to the supported

Table 1
Some physicochemical parameters of the supports and the catalysts studied.

Catalyst	% SiO_2	% MoO_3	% CoO	% MoO_3/Al_2O_3[a]	SSA of the support (m^2/g)	SSA of the catalyst (m^2/g)	p.z.c. of the support
1.5Si	1.5	17.0	2.0	17.5	220	164 (202)[b]	7.8
$1.5Si_{conv}$	1.5	17.0	2.0	17.5	220	154 (190)	7.8
10Si	10	15.5	2.0	17.3	322	230 (279)	6.7
20Si	20	13.8	2.0	17.0	340	242 (287)	6.0
$20Si_{conv}$	20	13.8	2.0	17.0	340	221 (262)	6.0
30Si	30	12.8	2.0	17.7	360	265 (311)	5.7

[a] MoO_3 loading of the alumina component.
[b] Values in parenthesis represent the specific surface area per gram of the support in the catalyst.

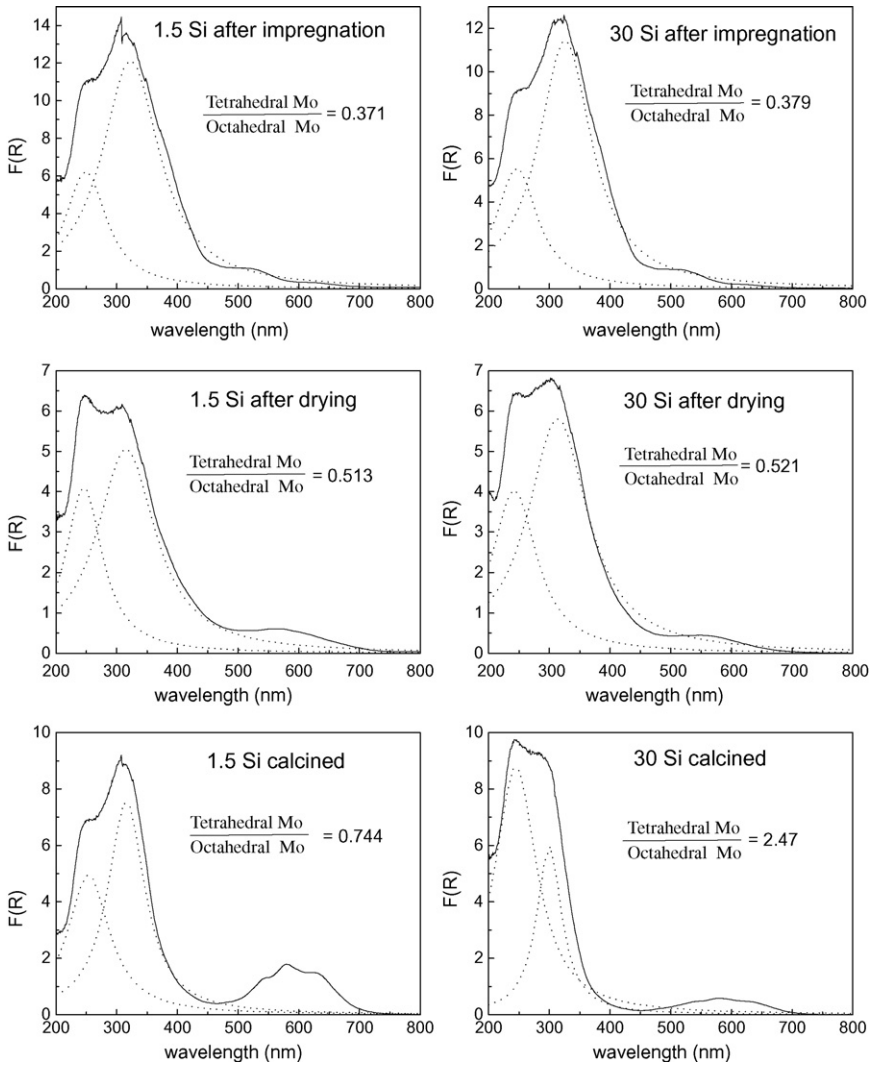

Fig. 4. Deconvolution of the wide absorption band appearing below 350 nm in the DR spectra of the samples 1.5Si and 30Si into two peaks centered at 265 and 305 nm. The preparation step and the tetrahedral to octahedral ratio of the Mo(VI) are indicated.

cobalt at tetrahedral symmetry ($CoAl_2O_4$) appears at about 600 nm [22]. The band at 425 nm and the shoulder at 750 nm due to the supported Co_3O_4 [22] do not appear in our DR spectra.

Inspection of Fig. 3 shows that the increase of the silica component in the mixed supports has two main effects: an increase of the intensity of the band at 265 nm at expense of the band at 305 nm and a decrease of the intensity of the triple band centered at about 600 nm.

The deconvoluted peaks centered at 265 and 305 nm of the DR spectra, recorded for the samples 1.5Si and 30Si after impregnation, drying and calcination, are illustrated in Fig. 4. Inspection of the "tetrahedral Mo/octahedral Mo" ratio, estimated using these peaks, shows that the values of this ratio increase with the temperature of the thermal treatment for both samples. These values are almost identical for both samples after impregnation and drying. However, they became different after calcination. The sample with the highest silica content exhibited the highest value. Moreover, inspection of this figure shows that the thermal treatment causes remarkable changes in the visible range of the spectrum. These changes reflect concomitant transformations in the supported cobalt species. Specifically, these changes indicate the progressive transformation of the supported aqua complex of Co(II) into supported $Co(OH)_2$ (after drying) and then into 'cobalt oxide' supported phase (after calcination).

The DR spectra of the conventional samples and the corresponding co-EDF ones are illustrated in Fig. 5.We observe that co-EDF favors the formation of supported cobalt at tetrahedral symmetry as it is manifested by the increase in the intensity of the triple band centered at about 600 nm.On the other hand, an interest-

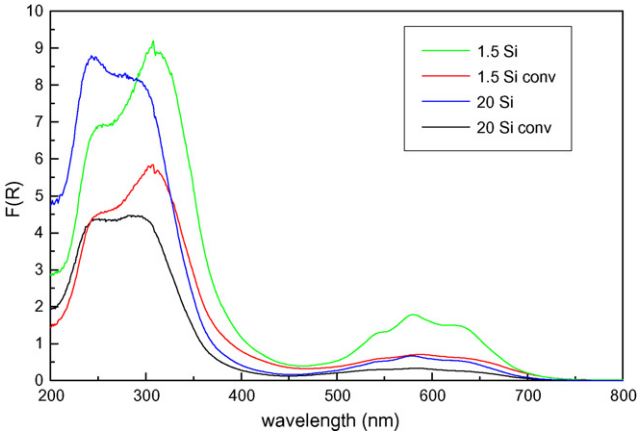

Fig. 5. Diffuse reflectance spectra recorded in the range 200–800 nm for the calcined conventional samples and the corresponding samples prepared by co-EDF.

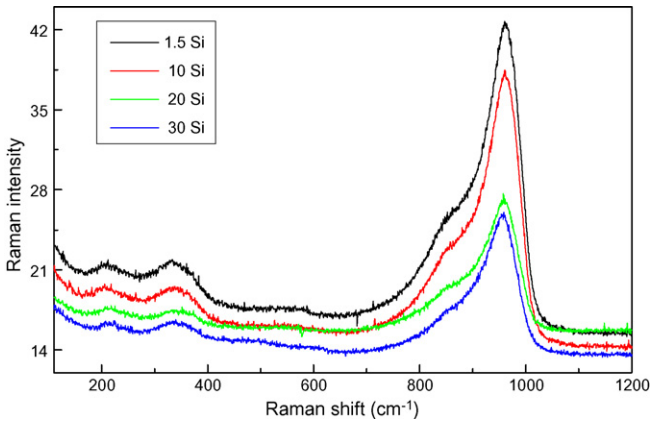

Fig. 6. Laser Raman spectra recorded for the calcined co-EDF samples in the range 120–1200 cm^{-1}.

ing observation is that the intensity of the bands at 240–270 and 290–320 nm due to the molybdenum species is considerably higher for the samples prepared by co-EDF compared to the corresponding conventional samples. Finally, it seems that the aforementioned effect of the silica content on the "tetrahedral Mo/octahedral Mo" ratio is more pronounced in the co-EDF samples.

3.5. Laser Raman spectroscopy

Three bands appear at 220, 300–400 and 800–1000 cm^{-1} in the LR spectra recorded in the range 200–1200 cm^{-1} for the calcined co-EDF samples (Fig. 6).

The band at 220 cm^{-1} is related to the presence of Mo–O–Mo bonds involved in the polymer Mo species [22,55–64]. The band at 300–400 cm^{-1} is comprised of two bands. The first centered at about 320 cm^{-1} is due to the tetrahedral Mo species, whereas the second centered at about 360 cm^{-1} indicates the presence of the octahedral Mo species [22,55–64]. Finally, the wide band at 800–1000 cm^{-1} may deconvoluted into three peaks centered at about 870, 930 and 960 cm^{-1}. The peaks at 930 and 960 cm^{-1} indicate, respectively, the presence of tetrahedral and octahedral Mo supported species whereas the wide peak at 870 reflects the formation of the Mo–O–Mo bonds involved in the polymer Mo species [64]. The aforementioned bands indicate the presence of well-dispersed Mo species on the surface of the mixed supports. The absence of an intense sharp peak at about 820 cm^{-1} point out the absence of MoO_3 supported nanocrystals [58,65]. Finally, the absence of a band at 696 cm^{-1} indicates that cobalt oxide is not formed on the surface of the mixed supports, implying well-dispersed cobalt species [66,67].

The deconvolution for the band appearing at 800–1000 cm^{-1} in the LR spectra (Fig. 6) is illustrated in Fig. 7.

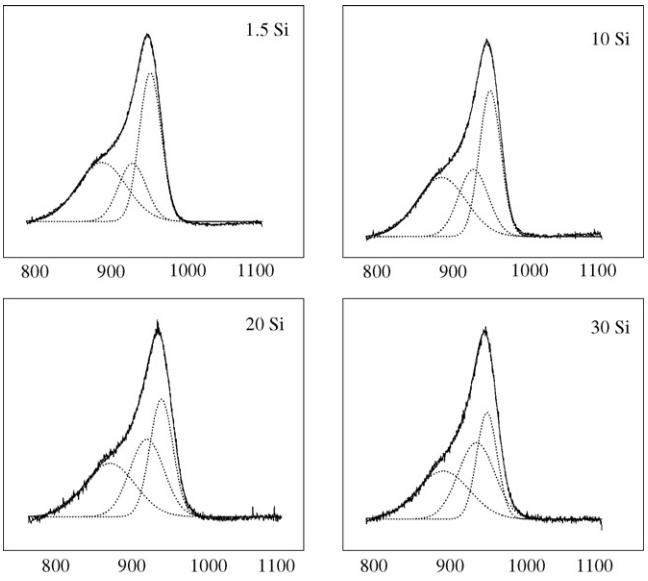

Fig. 7. Deconvolution of the band appearing at about 800–1000 cm^{-1} in the LR spectra (Fig. 6) into three peaks centered at about 870, 930 and 960 cm^{-1}.

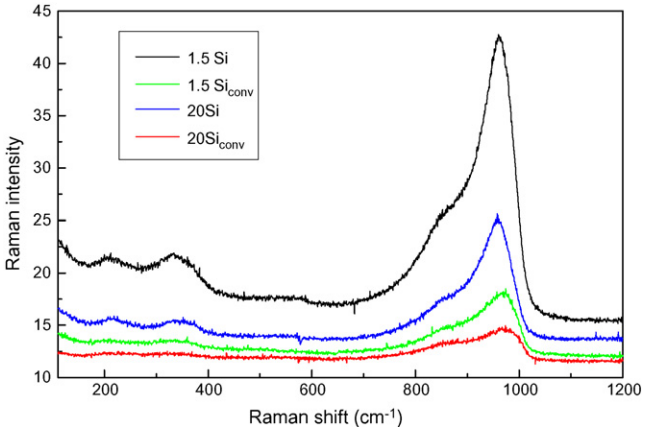

Fig. 8. Laser Raman spectra recorded in the range 150–1200 cm^{-1} for the calcined conventional samples and the corresponding samples prepared by co-EDF.

The increase of the silica component in the mixed supports brings about a decrease of the relative intensity of the peaks centered at 960 and 870 cm^{-1} with respect to the peak centered at 930 cm^{-1}.

The LR spectra recorded in the range 150–1200 cm^{-1} for the calcined CoMo-conventional samples and the corresponding samples prepared by co-EDF are illustrated in Figs. 8 and 9.

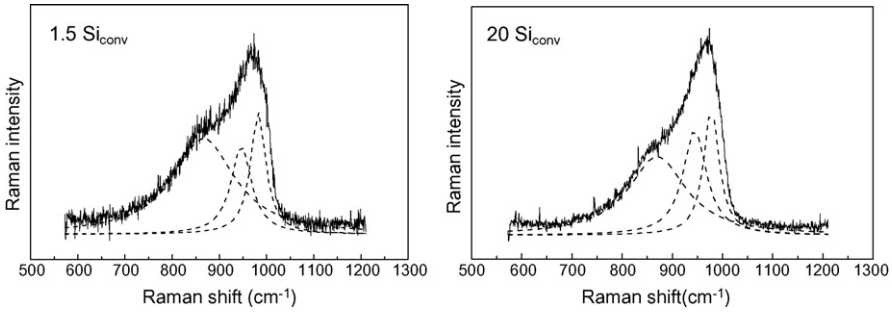

Fig. 9. Deconvolution of the band appearing at about 600–1000 cm^{-1} in the LR spectra for the samples prepared by conventional impregnation (Fig. 8) into three peaks centered at about 870, 940 and 970 cm^{-1}.

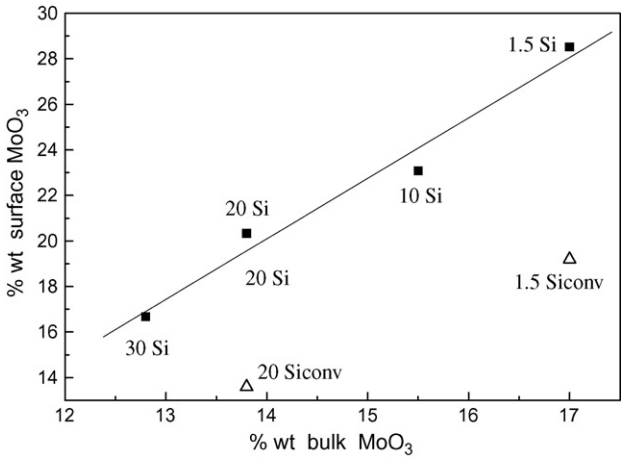

Fig. 10. Relationship between surface and bulk MoO_3 contents for the calcined samples.

The Raman spectra recorded for the conventional catalysts are similar to the corresponding ones recorded for the co-EDF catalysts indicating the presence of well-dispersed octahedral and tetrahedral Mo oxo-species in all samples. However, the main peak is slightly displayed at higher wavelengths (at 970 cm^{-1}) as compared to the EDF catalysts (at 960 cm^{-1}). This shift can be attributed to the higher degree of polymerization of the Mo phase in the catalysts prepared by conventional impregnation presumably indicating relatively low dispersion of the Mo(VI) supported phase with respect to that achieved in the corresponding co-EDF catalysts.

The intensity of the Raman peaks is much less intense for the conventionally prepared catalysts with respect to the co-EDF catalysts. It is well known that Raman spectroscopy cannot be considered as a surface sensitive technique. It is rather a semi-bulk technique. However, its probing depth, depending on the exciting irradiation, is about 20 nm.Thererfore, it rendered 'surface' sensitive for supported particles with size above this value. In view of the above and taking into account our XPS results (Section 3.6, Table 3, Fig. 10) we incline attributing the low intensity of the Raman peaks in the conventionally prepared catalysts to their relatively low Mo(VI) dispersion.

Likewise to that observed in the co-EDF samples, the increase of the silica content in the mixed support decreases the relative intensity of the peaks centered at 960 and 870 cm^{-1} with respect to the peak centered at 930 cm^{-1}. However, this effect is more intense in the co-EDF samples.

3.6. X-ray photoelectron spectroscopy

A very good separation of the peaks attributed to the $Mo3d_{5/2}$ and $Mo3d_{3/2}$ photoelectrons [22,35,36,68] was observed in the XP spectra of the Mo3d and Co2p photoelectrons recorded for the catalysts studied (not shown here). In contrast, the peaks due to the $Co2p_{1/2}$ and $Co2p_{3/2}$ [22] are rather poorly traced. The better definition of the Mo 3d peaks as compared to the Co 2p ones is mainly due to the different content of each of these elements and also due to the fact that the 2p signals of the late transition metals of the 3rd period are inherently weaker and extended on a larger spectral region than the 3d signal of the early transition metals of the 4th period.

The binding energies of the elements involved in the catalysts studied are illustrated in Table 2.

Inspection of Table 2 shows that the O1s binding energy shifts from the value corresponding to alumina to that corresponding to silica as the relative amount of the latter increases in the mixed support. This trend, if any, is not so clear for the specimens prepared by conventional impregnation. Similar values are obtained for the BE of the Al2p and Mo3d photoelectrons throughout the samples studied whereas the value obtained for the BE of the Co2p photoelectrons increases with the silica content in the support. The BE of the Co2p photoelectrons is lower for a sample prepared by conventional impregnation than that obtained for the corresponding co-EDF sample.

The surface compositions of the elements involved in the catalysts studied are illustrated in Table 3.

Let's first concentrate our attention to the surface composition obtained for the co-EDF catalysts. Inspection of Table 3 (rows 1, 3, 4 and 6) shows that the surface Mo concentration decreases as the silica content increases in the mixed supports whereas it remains practically constant with respect to the surface concentration of Al (7th column). In view of the above a linear dependence of the surface Mo concentration on the bulk one for the co-EDF catalysts is expected (Fig. 10). On the other hand, a slight increase in Co concentration was observed with Si content. Moreover, the expected increase (decrease) in the Si (Al) surface concentration was observed with the silica content in the mixed supports.

Let's compare the conventional with the co-EDF catalysts. Inspection of Table 3 and Fig. 10 shows that the surface Mo (Al) concentration is lower (higher) in the conventional than in the corresponding co-EDF catalysts. This is reflected in the considerably lower Mo/Al surface ratio obtained for the conventional samples. In contrast, the surface concentration of Co is relatively high in the conventional samples.

3.7. Temperature-programmed desorption of ammonia

The temperature-programmed desorption curves of ammonia adsorbed on the surface of the mixed supports and of the co-EDF

Table 3
Surface composition (% atoms) of the catalysts calculated taking into account the number of scans and the atomic sensitivity factors of each element [35].

Catalyst	Mo	Co	Al	Si	O	$\frac{Mo}{Al}$
1.5Si	4.7	0.53	34.7	–	60.0	0.136
$1.5Si_{conv}$	3.8	0.75	45.1	–	50.3	0.083
10Si	3.7	0.56	27.0	8.9	59.8	0.138
20Si	3.1	0.57	21.2	9.9	65.1	0.149
$20Si_{conv}$	2.9	0.70	35.2	14.2	47.0	0.079
30Si	2.6	0.59	18.1	15.6	63.1	0.142

Table 2
Binding energies[a] for the elements present on the surface of the catalysts studied.

Catalyst	Al2p binding energy/eV	O1s binding energy/eV	Co2p binding energy/eV	Mo3d binding energy/eV		Si2p binding energy/eV
1.5Si	74.7	532.0	782.3	233.3	236.0	–
$1.5Si_{conv}$	74.9	531.9	781.3	233.4	236.0	–
10Si	74.9	532.3	782.3	233.5	236.6	103.1
20Si	75.0	532.8	783.1	233.9	236.7	103.7
$20Si_{conv}$	75.0	532.1	782.6	233.6	236.1	103.5
30Si	74.9	532.8	783.7	233.5	236.6	103.4

[a] C1s peak centered at 285.5 eV was used for referencing the binding energies.

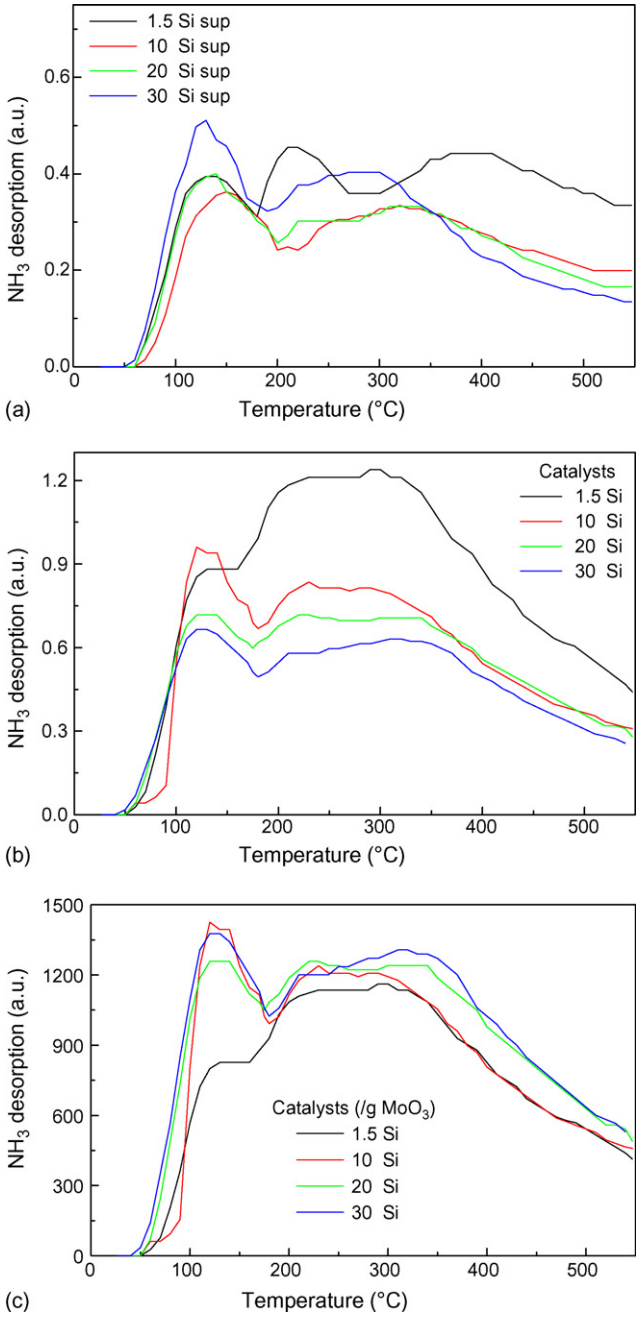

Fig. 11. Temperature-programmed desorption curves of ammonia adsorbed on the surface of the mixed supports (a) and of the co-EDF catalysts studied (b, c). The amount of the desorbed ammonia in Fig. 11a and b was expressed per m^2 of the mixed support whereas this amount was expressed per gram of the supported MoO_3 phase in Fig. 11c.

catalysts are illustrated in Fig. 11a and b, respectively. In these figures the amount of the desorbed ammonia was expressed per m^2 of the mixed support. The temperature-programmed desorption curves of ammonia adsorbed on the surface of the co-EDF catalysts are also illustrated in Fig. 11c. In this figure the amount of the desorbed ammonia was expressed per gram of the supported MoO_3 phase. The low temperature desorption peak (120–150 °C) is assigned to the Bronsted acid sites which are developed on the surface [69–73]. The second wide desorption peak, extended in the range 200–550 °C, may be partly attributed to the relatively strong Bronsted acid sites (200–380 °C) and partly to Lewis acid sites (380–550 °C) [70].

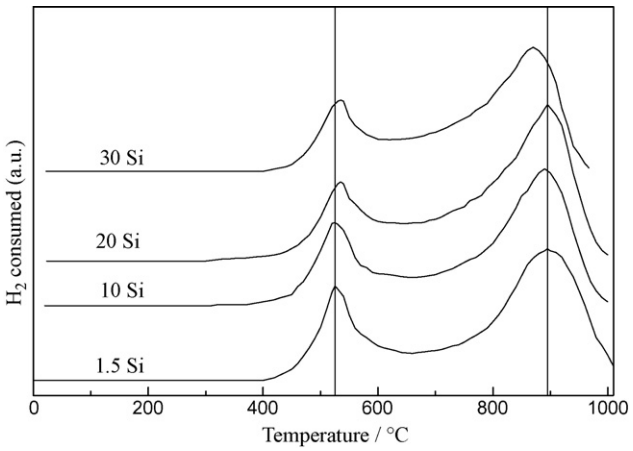

Fig. 12. Temperature-programmed reduction curves of the co-EDF catalysts studied. The symbols of the catalysts are indicated.

An increase of the area under the desorption peaks at 120–150 °C and 200–380 °C with the silica content has been observed for the pure supports. The only exception is the 1.5Si sup mixed support. In contrast, the area under the desorption peak at 380–550 °C was decreased with the silica content. The deposition of the cobalt–molybdenum phase generally causes a considerable increase of the area under the first and the second peak (compare Fig. 11a with Fig. 11b).

3.8. Temperature-programmed reduction

The temperature-programmed reduction curves of the co-EDF catalysts studied are illustrated in Fig. 12. Two peaks appear at about 530 and 900 °C. These are typical of well-dispersed molybdenum supported species. The low temperature peak is attributed to the partial reduction of Mo(VI) to Mo(IV) of amorphous, highly defective, multilayered oxides (octahedral Mo species) [69,74]. The high temperature peak is attributed to the deep reduction of all Mo species, including the highly dispersed tetrahedral (monomer) Mo(VI) oxo-species [69,74]. The absence of additional reduction peaks at c.a. 600–650 and 350 °C indicate, respectively, that MoO_3 and cobalt oxide supported crystallites are not formed on the supports surface [74–77].

The temperatures corresponding to the reduction peaks and the magnitudes of these peaks are not changed considerably with the silica component in the mixed supports.

The temperature-programmed reduction curves of the catalysts prepared following the conventional procedure and the corresponding co-EDF catalysts are illustrated in Fig. 13. We observe that the intensity of the reduction peaks achieved for the conventional samples is smaller than that achieved for the corresponding co-EDF samples. Moreover, the low temperature peaks of the conventional samples are slightly displayed to higher temperatures. Both observations indicate that the Mo supported phase (mainly responsible for the appearance of the reduction peaks) is less reducible in the conventional than in the corresponding co-EDF samples.

3.9. NO chemisorption

The values of the NO uptake of the sulfided catalysts are compiled in Table 4. It is known that the NO uptake is a good estimate of the concentration of the HDS "active sites" namely, of the concentration of the "sulphur vacancies" of the MoS_2 slabs decorated by supported cobalt.

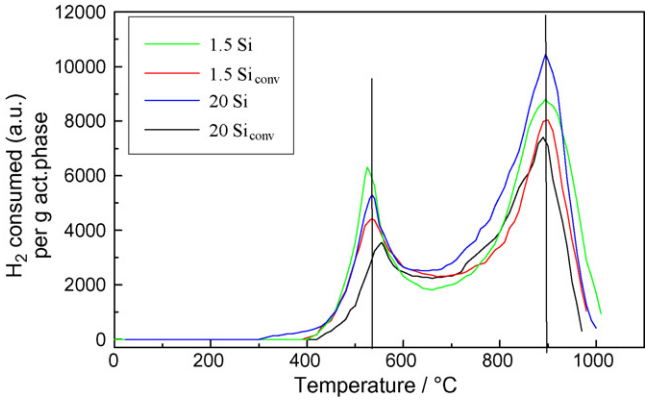

Fig. 13. Temperature-programmed reduction curves of the conventional and the corresponding co-EDF catalysts. The consumption of hydrogen is expressed (in a.u.) per gram of active phase.

Table 4
Chemisorption of NO on the sulfided catalysts.

Catalyst	μmol NO/g MoO_3
1.5Si	496.8
1.5Si$_{conv}$	472.2
10Si	483.1
20Si	730.4
20Si$_{conv}$	701.3
30Si	693.4

The NO uptake for the co-EDF samples (rows 1, 3, 4 and 6) follows a zigzag trend (20Si > 30Si > 1.5Si > 10Si) depending on the silica content in the mixed supports. It takes its maximum value for the sample containing 20% SiO_2 in the corresponding mixed support. The values obtained for the conventional samples (rows 2 and 5) are lower than the ones obtained for the corresponding co-EDF samples (rows 1 and 4).

3.10. Catalytic behavior

The rates of hydrodesulphurization of thiophene determined at three different temperatures over the co-EDF catalysts are illustrated in Fig. 14.

Inspection of this figure shows that the rate depends on the silica content in the mixed supports following the zigzag trend: 20Si > 30Si > 1.5Si > 10Si. It takes its maximum value for the sample containing 20% SiO_2 in the corresponding mixed support. The selectivity determined is not considerably different over the catalysts studied.

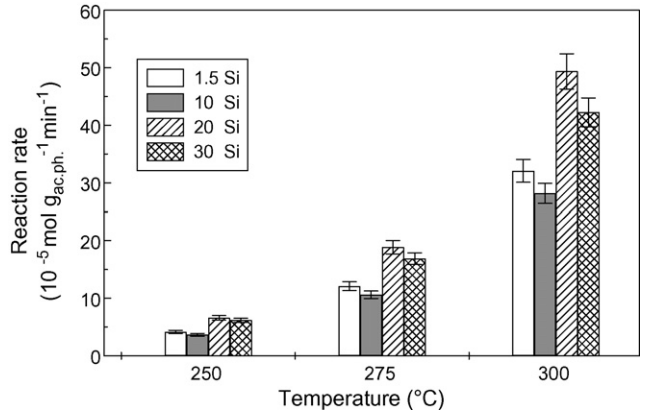

Fig. 14. The rates of the hydrodesulphurization of thiophene determined at three temperatures over the co-EDF catalysts prepared. The rates are expressed per gram of the supported phase. The symbols of the catalysts are indicated.

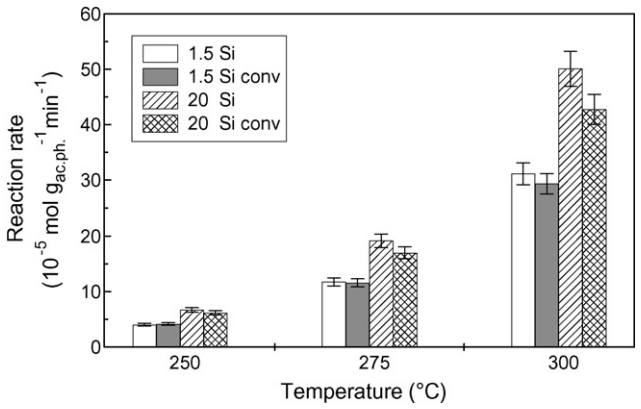

Fig. 15. The rates of the hydrodesulphurization of thiophene determined at three temperatures over two co-EDF catalysts and the corresponding ones prepared by the conventional incipient wetness impregnation. The rates are expressed per gram of the supported phase. The symbols of the catalysts are indicated.

The rates of the hydrodesulphurization of thiophene determined at three different temperatures over the catalysts 1.5Si, 1.5Si$_{conv}$, 20Si and 20Si$_{conv}$ are illustrated in Fig. 15. Concerning the catalysts prepared by the conventional incipient wetness impregnation the most active is the sample 20Si$_{conv}$. Moreover, we observe that the co-EDF catalysts are more active than the corresponding ones prepared by incipient wetness impregnation. Again, the selectivity determined is not considerably different over the catalysts studied.

4. Discussion

4.1. Location of the Mo(VI) and Co(II) species on the mixed supports in the co-EDF catalysts

4.1.1. A patch-wised surface model for the mixed support

The porous grains of the Al_2O-SiO_2 mixed supports are comprised of interconnected alumina and silica nanoparticles. Therefore, the surface of a mixed grain can be considered as the alumina surface interrupted by silica patches. This patch-wised surface model seems to be quite realistic for the samples 10Si, 20Si and 30Si. In contrast, the Si atoms are presumably incorporated inside the alumina matrix in the sample with the minimum silica content (1.5Si). This is in agreement to the surface composition determined by XPS (Table 3). Moreover, this would justify the aforementioned abnormal TPD behavior of the 1.5Si support and 1.5Si co-EDF catalyst (Fig. 11). An approximate estimation of the relative extent of the alumina and silica surface regions could be obtained by inspecting the surface atomic composition of the co-EDF catalysts regarding the Al and Si atoms (Table 3). The increase, with the silica content, of the silica surface regions in the whole surface of the mixed supports is also reflected to the progressive decrease of the p.z.c. values from the 1.5Si to the 30Si mixed support (Table 1). The aforementioned patch-wised surface model is a useful approximation which does not exclude that a small part of the Si is incorporated into the alumina lattice or forms another type of mixed phase.

4.1.2. Location of the Mo(VI) species

The Al_2O_3-SiO_2 supported CoMo catalysts studied so far were prepared by incipient wetness impregnation or incipient co-impregnation. In this case one cannot expect selective location of the aforementioned nanoparticles. In contrast, by applying the co-EDF technique and selecting properly the impregnation parameters we are able *to direct selectively* the Mo(VI) species on the

alumina surface. This is because the Mo(VI) oxo-species(MoO_4^{2-} and $Mo_7O_{24}^{6-}$ [42,43]) are negatively charged under our experimental conditions whereas the alumina and silica surface regions are positively and negatively charged, respectively. The selective location of the Mo(VI) oxo-species on the alumina surface regions is corroborated by the deposition isotherms, (Fig. 1), in conjunction with the absence of yellow color, characteristic of the silicomolybdenic acid [44,45]. This is also in line with the observation that the MoO_3 content of the catalysts decreases as the alumina content decreases, whereas it remains practically constant with respect to the alumina content of the support (Table 1). Moreover, it is in agreement with the constant Mo/Al surface atomic ratio (Table 3) and that the "tetrahedral Mo/octahedral Mo" ratio, determined just after impregnation (Fig. 4), is independent of the silica content.

4.1.3. Location of the Co(II) species

Both alumina and silica adsorb the $[Co(H_2O)_6]^{2+}$ aqua complex present in the aqueous solution (Fig. 2). The deposition mechanism involves the replacement one or more of the water ligands with the γ-alumina surface oxygen atoms and the formation of inner sphere complexes [20,48–50]. As to the silica it is not yet clear whether the deposition involves the formation of inner sphere complexes or takes place through electrostatic adsorption [20,49].

The relative distribution of Co(II) between the alumina and silica surface regions is determined by two opposite factors: the relatively high Co(II) adsorptivity of silica (Fig. 2) and the selective deposition of Mo(VI) oxo-species on the alumina surface regions which decreases the positive charge at the 'alumina/electrolytic solution interface' facilitating the deposition of the $[Co(H_2O)_6]^{2+}$ aqua complexes [77]. The formation of negatively charged Co–Mo complexes in the impregnating solution [78] favors also Co(II) deposition on alumina regions.

The increase of the silica content in the mixed supports favors the Co(II) deposition on the silica regions at the expense of the Co(II) deposition on the alumina surface regions. This presumably results in the decrease of the amount of the catalytically inactive cobalt aluminate. The latter could be inferred from the decrease in the intensity of the triple band centered at about 600 nm with increasing SiO_2 content in the co-EDF catalysts (Fig. 3). The deposition of the Co(II) species on the surface regions exposed by both components of the mixed supports could also be concluded by the observation that the CoO loading remains practically constant whereas the surface atomic concentration of Co(II) increases slightly with the silica content of the support.

4.2. The nature and the state of dispersion of the supported Mo(VI) and Co(II) species in the co-EDF catalysts

4.2.1. Nature of the supported Mo(VI) species

The increase, with the silica content, in the intensity of the band at 265 nm at expense of the band at 305 nm in the DR spectra (Fig. 3) and the decrease of the relative intensity of the peaks centered at 960 and 870 cm^{-1} with respect to the peak centered at 930 cm^{-1} in the Raman spectra (Fig. 7), clearly show that the increase of the silica patches in the patch-wised surface favors the formation of the monomer species in the catalysts.

Inspection of Fig. 4 clearly shows that the "tetrahedral Mo/octahedral Mo" ratio achieved just *after impregnation* is independent of the silica content. This is expected taking into account that the Mo(VI) species are deposited exclusively on the alumina surface. In the drying step this ratio increases considerably in both samples. This is because the pH increases upon evaporation taking initially the p.z.c. value of the support and finally the p.z.c. of the γ-alumina above the alumina surface regions. This causes transformation of the polymer into monomer surface species. Taking into account the exclusive deposition on the alumina surface it is conceivable why the extent of the aforementioned transformation is independent of the silica content in the mixed support. The aforementioned transformation further proceeds after calcination. In this step the promotion exerted by the silica component is obvious. We have not for the moment a plausible explanation for this effect.

4.2.2. Dispersion of the supported Mo(IV) and Co(II) species

Our experimental data show the absence of MoO_3 supported nanoparticles indicating a good Mo(VI) dispersion. The most important evidences are the peaks appearing at about 530 and 900 °C in the TPR curves (Fig. 12) as well as the absence of peaks due to the MoO_3 nanoparticles in the diffraction patterns, the absence of an intense sharp peak at about 820 cm^{-1} in the Raman spectra (Fig. 6) and the absence of a reduction peak at ca. 600–650 °C in TPR curves (Fig. 12). The linear relationship observed in Fig. 10 between the bulk and the surface Mo concentration clearly shows that this good dispersion is practically constant, irrespectively of the silica content in the mixed support.

The absence of a reduction peak at ca. 350 °C (Fig. 12) and of a band at 650–700 cm^{-1} in the Raman spectra (Fig. 6) indicates the absence of supported 'three-dimensional' cobalt oxide suggesting a very good Co(II) dispersion.

The very good dispersion obtained for the Mo(VI) and Co(II) supported species are in line with the observation that the decrease in the specific surface area of the mixed support due to the deposition of the Mo(VI) and Co(II) species is rather small (8–15.5%, Table 1 values in parenthesis). This very good dispersion is the result of the deposition mode (adsorption, surface reaction) imposed by the application of the co-EDF impregnation technique versus the bulk precipitation mode largely, but not exclusively, imposed by the conventional impregnation technique.

4.3. On the acidity of the mixed supports and co-EDF catalysts

The decrease in the p.z.c. value with the silica content (Table 1) indicates that the presence of SiO_2 increases the Bronsted acidity of the mixed supports. This is also inferred by the corresponding increase of the area under the desorption peaks at 120–150 °C and 200–380 °C (Fig. 11a). In contrast, the decrease in the area under the desorption peak appearing in the region 380–550 °C indicates that the silica component decreases the Lewis acidity of the mixed supports. This is in rather good agreement with literature. In fact, La Parola et al. [26] investigated the Bronsted and Lewis acidity of silica–alumina mixed supports on the base of IR spectra of adsorbed pyridine and found that the ratio of the Lewis to Bronsted sites decreases with increasing the silica content. As already mentioned, the deposition of the cobalt–molybdenum phase generally caused a considerable increase in the whole acidity reflected to the increase of the area under the first and the second peak (Fig. 11b). It seems that the intensity of the effect increases with the Mo content of the catalyst, which is inversely proportional to the amount of silica in the mixed support. In fact, the acidity expressed per gram of the supported MoO_3 phase (Fig. 11c) is practically constant. The only exception is the 1.5Si catalyst. The above indicates that the supported molybdenum oxo-species create surface acid sites presumably related with oxygen atoms bound to molybdenum.

4.4. The influence of the alumina-silica composition on the catalytic activity in the co-EDF catalysts

As already mentioned the HDS activity of the catalysts prepared by co-EDF follows the trend: 20Si > 30Si > 1.5Si > 10Si (Fig. 14). The same trend follows the number of "active sites" as it was estimated by the NO adsorption (Table 4). We have, therefore, to explain this

rather complicated (zigzag) trend. This trend shows that two, at least, opposite factors, related to the composition of the mixed support, influence the HDS activity. The dispersion of the Mo(VI) is constant (Fig. 10). On the other hand the total acidity of the catalysts expressed per gram of the active phase is not changed considerably with the support composition (Fig. 11c). Thus, the aforementioned parameters do not seem to be relevant to the HDS activity trend.

There are two other parameters which should be investigated. The first is the ratio "tetrahedral (monomer) /octahedral (polymer) Mo species". As already mentioned, this ratio increases monotonically with the amount of the silica component in the mixed support. This increment is expected to bring about a decrease in the catalytic activity, because the tetrahedral (monomer) species, interacted relatively strong with the alumina surface, are harder reducible/sulphidable resulting in rather small and not very active MoS_2 slabs. The second parameter is the amount of the catalytically inactive cobalt aluminate. This generally decreases with the increase of the silica component in the mixed support (Fig. 3). The way by which the silica component protects the supported cobalt by inhibiting the formation of the cobalt aluminate has been explained. Furthermore, we assume that the cobalt supported on silica surface regions participates in the formation of the HDS active sites equally well with that supported on the γ-alumina surface regions either by distance (remote control model) [79] or by approaching (*via* surface diffusion) and decorating the MoS_2 supported γ-alumina slabs (CoMoS model) [80]. In any case the combination of a coordinative unsaturated site in the slab with the supported cobalt constitutes the HDS active site. These sites are also titrated by the chemisorbed NO (Table 4).

The increase of the silica content from 1.5 to 10% increases considerably the ratio "tetrahedral (monomer)/octahedral (polymer) species" (Figs. 3 and 7) whereas it slightly decreases the amount of cobalt aluminate (Fig. 3). Therefore, the combined influence of these changes results in a decrease in the HDS activity (Fig. 14). The increase of the silica content from 10 to 20% increases the ratio "tetrahedral (monomer) /octahedral (polymer) Mo species" (Figs. 3 and 7) whereas it markedly decreases the amount of cobalt aluminate (Fig. 3). These bring about an increase to the catalytic activity (Fig. 14). The additional increase in the amount of the silica component of the mixed support from 20 to 30% increases further the ratio "tetrahedral (monomer) /octahedral (polymer) Mo species" (Figs. 3 and 7) but it does not affect the amount of cobalt aluminate (Fig. 3) resulting thus in a decrease in the catalytic activity (Fig. 14). In summary, the combined change in the ratio "tetrahedral (monomer) /octahedral (polymer) Mo species" and in the amount of the cobalt aluminate brought about by changing the composition of the Al_2O_3-SiO_2 support determines the trends observed in the catalytic activity of the co-EDF catalysts.

4.5. The influence of the preparation method on surface characteristics and catalytic activity

The most important result of the present work is that the co-EDF catalysts are more active than the corresponding catalysts prepared by conventional impregnation (Fig. 15). First, this concerns the catalyst with the minimum silica content and confirms the beneficial application of the co-EDF technique reported for the catalysts prepared on pure γ-alumina [21–23]. Moreover, this concerns the co-EDF catalyst with the maximum activity (20Si) and shows that the combination of a proper impregnation technique with a mixed Al_2O_3-SiO_2 support of suitable composition may be proved fruitful for improving further the HDS activity.

In view of the considerations of the previous subsection it seems that three parameters mainly affect catalytic behavior, namely the amount of the catalytically inactive cobalt aluminate, the Mo tetrahedral/octahedral ratio and obviously the dispersion of the active phase (principally of the molybdenum phase).

The replacement of the conventional impregnation procedure by the co-EDF methodology causes a rather undesirable effect regarding the first parameter. In fact, co-EDF favors the formation of supported cobalt at tetrahedral symmetry as it is manifested by the increase in the intensity of the triple band centered at about 600 nm (Fig. 5). This is rather expected because following the conventional procedure cobalt species are deposited on the surface of the *already supported Mo phase* rather than on the bare support surface. This prevents the interaction of the Co phase with the alumina surface diminishing the dilution of cobalt ions into the γ-alumina lattice. In contrast, following co-EDF cobalt is deposited, simultaneously with the molybdenum, on the support surface. The effect is not so pronounce in the sample rich in silica (Fig. 5) because in this case a considerable portion of cobalt is deposited on the silica surface regions. The decreasing formation of cobalt aluminate in the conventional samples could explain the relatively high surface Co concentration in these samples (Table 3) as well as the observation that the value of BE observed for the Co2p photoelectrons is lower for a sample prepared by conventional impregnation than that obtained for the corresponding co-EDF sample (Table 2).

The replacement of the conventional impregnation procedure by the co-EDF methodology does not influence considerably the Mo tetrahedral/octahedral ratio though it seems favoring somewhat the tetrahedral Mo species (Fig. 5).

The use of the co-EDF technique instead of the conventional procedure increases the dispersion of the Mo(VI) precursor phase. It is directly resulted by the observation that the surface Mo (Al) concentration achieved is markedly higher (lower) in the co-EDF catalysts than in the corresponding conventional ones (Table 3). This is reflected in the considerably higher Mo/Al surface ratio obtained for the co-EDF samples (Table 3). The relatively high dispersion of the Mo(VI) supported phase following EDF is also inferred by the observation that the decrease in the specific surface area after the deposition of the CoMo phase, drying and calcination is more pronounced in the conventional samples (Table 1) than in the co-EDF counterparts as well as by the observation that the intensity of the bands at 240–270 and 290–320 nm due to the molybdenum species is considerably higher for the samples prepared by co-EDF compared to the corresponding conventional samples (Fig. 5).The lower Mo(VI) dispersion obtained in the conventional samples is also suggested by the displacement of the main LR peak at higher wavelengths as compared to the EDF catalysts (Section 3.5, Fig. 8). The above results, being in line with literature [18–23], show that the co-EDF technique results in catalysts with better dispersion of the Mo(VI) supported phase, irrespectively of the support used.

In particular, in the mixed supports studied here the co-EDF procedure directs the Mo deposition on the γ-alumina surface regions where a high dispersion of the molybdenum phase is obtained. In contrast, using the conventional incipient wetness impregnation technique the molybdenum phase is deposited on both components. In that case a relatively low Mo dispersion is expected. In fact, as already mentioned Massoth et al. [25] reported monolayer dispersion over pure alumina or low silica containing Al_2O_3-SiO_2 supports and formation of three-dimensional crystallites of the Mo supported phase in the high silica containing Al_2O_3-SiO_2 supports. The achievement of the better dispersion of the molybdenum phase on the γ-alumina surface regions compared to that obtained on the silica patches was also reported by La Parola et al. [26].

The well-dispersed Mo(VI) species obtained in the 1.5Si and 20Si catalysts are more reducible than the corresponding ones obtained in the conventional $1.5Si_{conv}$ and $20Si_{conv}$ catalysts (Section 3.8, Fig. 13). This can be attributed to the better dispersion of the Mo(VI) species in the co-EDF samples, in agreement to the XPS results. The

well-dispersed Mo(VI) phase in the EDF samples provides, upon hydrogenation/sulphidation, a high number of active sites as it was estimated by NO adsorption (Table 4).

In conclusion, the replacement of the conventional impregnation procedure by the co-EDF methodology increases the dispersion and the reducibility of the Mo(IV) supported phase and thus the population of the active sites. These over-compensate the increasing formation of cobalt aluminate and explain why the co-EDF catalysts are more active than the corresponding catalysts prepared by conventional impregnation.

5. Conclusions

By applying co-EDF and selecting the proper impregnation parameters it was feasible to deposit the Mo(VI) species exclusively on the γ-alumina surface regions of Al_2O_3-SiO_2 mixed supports where a relatively high dispersion of the molybdenum supported phase has been achieved. Thus, this technique provided more active catalysts than the conventional impregnation procedure. The partition of the Co(II) species on both surface regions protected a part of the Co(II) phase inhibiting the formation of the catalytically inactive cobalt aluminate. The increase of the silica component in the mixed support has two main effects: the aforementioned decrease in the amount of cobalt aluminate and the increase of the ratio "tetrahedral (monomer)/octahedral (polymer) species". The combined influence of these parameters on activity explained the zigzag trend (20Si > 30Si > 1.5Si > 10Si) achieved regarding the HDS activity over the catalysts prepared by co-EDF.

References

[1] B. Delmon, Catal. Lett. 22 (1993) 1–32.
[2] I. Iwamoto, J. Grimblot, Adv. Catal. 44 (2000) 417.
[3] H.K. Matralis, A. Lycourghiotis, P. Grange, B. Delmon, Appl. Catal. 38 (1988) 273.
[4] L. Ding, Z. Zhang, Y. Zheng, Z. Ring, J. Chen, Appl. Catal. A: Gen. 301 (2006) 241.
[5] C.J. Song, C. Kwak, S.H. Moon, Catal. Today 74 (2002) 193.
[6] H. Kim, J.J. Lee, J.H. Koh, S.H. Moon, Appl. Catal. B: Environ. 50 (2004) 17.
[7] A. Usman, T. Kubota, Y. Araki, K. Ishida, Y. Okamoto, J. Catal. 227 (2004) 523.
[8] B. Pawelec, T. Halachev, A. Olivas, T.A. Zepeda, Appl. Catal. A: Gen. 348 (2008) 30.
[9] F. Dumeignil, K. Sato, M. Imamura, N. Matsubayashi, E. Payen, H. Shimada, Appl. Catal. A: Gen. 315 (2006) 18.
[10] R. Cattaneo, F. Rota, R. Prins, J. Catal. 199 (2001) 318.
[11] R. Cattaneo, T. Shido, R. Prins, J. Catal. 185 (1999) 199.
[12] V. Sundaramurthy, A.K. Dalai, J. Adjaye, Catal. Lett. 102 (2005) 299.
[13] J.A.R. van Veen, E. Gerkema, A.M. van der Kraan, Arie Knoester, J. Chem. Soc., Chem. Commun. (1987) 1684.
[14] L. Medici, R. Prins, J. Catal. 163 (1996) 38.
[15] L. Coulier, V.H.J. de Beer, J.A.R. van Veen, J.W. Neimantsverdriet, J. Catal. 197 (2001) 26.
[16] R. Cattaneo, T. Weber, T. Shido, R. Prins, J. Catal. 191 (2000) 225.
[17] L. Coulier, Top. Catal. 13 (2000) 99.
[18] Ch. Papadopoulou, L. Karakonstantis, H.K. Matralis, Ch. Kordulis, A. Lycourghiotis, Bull. Soc. Chim. Belg. 105 (1996) 247.
[19] K. Bourikas, H.K. Matralis, Ch. Kordulis, A. Lycourghiotis, J. Phys. Chem. 100 (1996) 11711.
[20] K. Bourikas, Ch. Kordulis, A. Lycourghiotis, Catal. Rev. 48 (2006) 363.
[21] Ch. Kordulis, A.A. Lappas, Ch. Fountzoula, K. Drakaki, A. Lycourghiotis, I.A. Vasalos, Appl. Catal. A: Gen. 209 (2001) 85.
[22] Ch. Papadopoulou, J. Vakros, H.K. Matralis, Ch. Kordulis, A. Lycourghiotis, J. Colloid Interf. Sci. 261 (2003) 146.
[23] Ch. Papadopoulou, J. Vakros, H.K. Matralis, G.A. Voyiatzis, Ch. Kordulis, J. Colloid Interf. Sci. 274 (2004) 159.
[24] F.E. Massoth, G. Muralidhar, J. Shabtai, J. Catal. 85 (1994) 44.
[25] F.E. Massoth, G. Muralidhar, J. Shabtai, J. Catal. 85 (1994) 52.
[26] V. La Parola, G. Deganello, A.M. Venezia, Appl. Catal. A: Gen. 260 (2004) 237.
[27] Kh. Al-Dalama, A. Stanislaus, Energy & Fuels 20 (2006) 1777.
[28] J. Ramirez, R. Contreras, P. Castillo, Appl. Catal. A: Gen. 197 (2000) 69.
[29] M. Hussain, S. Ki Song, J. Hee Lee, S. Ki Ihm, Ind. Eng. Chem. Res. 45 (2006) 536.
[30] M. Souza, B.A. Marinkovic, P.M. Jardim, A.S. Araujo, A.M.G. Pedrosa, R.R. Souza, Appl. Catal. A: Gen. 316 (2007) 212.
[31] T.A. Zepeda, B. Pawelec, J.L.G. Fierro, A. Olivas, S. Fuentes, T. Halachev, Micr. Mesop. Mater. 111 (2008) 157.
[32] F.D. Snell, Photometric and Fluorometric Methods of Analysis of Metals, Vol. 2, Wiley, New York, 1984, p. 1296.
[33] E.B. Samdell, Colorimetric Determination of Traces of Metals, Interscience, New York, 1950, p. 274.
[34] L. Karakonstantis, Ch. Kordulis, A. Lycourghiotis, Langmuir 8 (1992) 1318.
[35] C.D. Wagner, W.M. Riggs, L.E. Davis, J.F. Moulder, G.E. Mullenberg, Handbook of X-Ray Photoelectron Spectroscopy, Perkin–Elmer, 1978.
[36] C.D. Wagner, L.E. Davis, M.V. Zeller, J.A. Taylor, R.H. Raymond, L.H. Gale, Surf. Interface Anal. 3 (1981) 211.
[37] J.L. Lemaitre, in: F. Delannay (Ed.), Characterization of Heterogeneous Catalysts, Marcel Dekker Inc., New York and Basel, 1984, Chapter 2.
[38] I. Georgiadou, C. Papadopoulou, H.K. Matralis, G.A. Vogiatzis, A. Lycourghiotis, C. Kordulis, J. Phys. Chem. B 102 (1998) 8459.
[39] J. Vakros, Ch. Kordulis, A. Lycourghiotis, Chem. Comm. (2002) 1980.
[40] K. Bourikas, J. Vakros, Ch. Kordulis, A. Lycourghiotis, J. Phys. Chem. B 107 (2003) 9441.
[41] J. Vakros, Ch. Kordulis, Appl. Catal. A: Gen. 217 (2001) 287.
[42] N. Spanos, L. Vordonis, Ch. Kordulis, A. Lycourghiotis, J. Catal. 124 (1990) 301.
[43] N. Spanos, A. Lycourghiotis, J. Catal. 147 (1994) 57.
[44] J.A.R. Van Veen, P.A.J.M. Hendriks, Polyhedron 5 (1986) 75.
[45] P. Sarrazin, S. Kasztelan, E. Payen, J.P. Bonnelle, J. Grimblot, J. Phys. Chem. 97 (1993) 5954.
[46] L. Vordonis, N. Spanos, P.G. Koutsoukos, A. Lycourghiotis, Langmuir 8 (1992) 1736.
[47] N. Spanos, A. Lycourghiotis, J. Chem. Soc. Faraday Trans. 89 (1993) 4101.
[48] J. Vakros, K. Bourikas, S. Perlepes, Ch. Kordulis, A. Lycourghiotis, Langmuir 20 (2004) 10542.
[49] K. Bourikas, Ch. Kordulis, J. Vakros, A. Lycourghiotis, Adv. Colloid Interf. Sci. 110 (2004) 97.
[50] Th. Ataloglou, K. Bourikas, J. Vakros, Ch. Kordulis, A. Lycourghiotis, J. Phys. Chem. B 109 (2005) 4599.
[51] L. Vordonis, Ch. Kordulis, A. Lycourghiotis, J. Chem. Soc., Faraday Trans. I 84 (1988) 1593.
[52] J. Vakros, K. Bourikas, Ch. Kordulis, A. Lycourghiotis, J. Phys. Chem. B 107 (2003) 1804.
[53] L.G.A. Van De Water, J.A. Bergwerff, B.G. Leliveld, B.M. Weckhuysen, K.P. De Jong, J. Phys. Chem. B 109 (2005) 14513.
[54] L.G.A. Van De Water, J.A. Bergwerff, T.A. Nijhuis, K.P. De Jong, B.M. Weckhuysen, JACS 127 (2005) 5024.
[55] G. Mestl, T.K.K. Srinivasan, Catal. Rev. Sci. Eng. 40 (1998) 451.
[56] J.M. Stencel, Raman Spectroscopy for Catalysis, Van Nostrand Reinhold, New York, 1990, pp. 69–75.
[57] J.A. Bergwerff, M. Jansen, B.R.G. Leliveld, T. Visser, K.P. De Jong, B.M. Weckhuysen, J. Catal. 243 (2006) 292.
[58] M. Del Arco, S.R.G. Carrazan, C. Martin, V. Rivew, J.V. Garcia-Ramos, P. Carmona, Spectrochim. Acta Part A 50 (1994) 2215.
[59] S.D. Kohler, J.G. Ekerdt, D.S. Kim, I.E. Wachs, Catal. Lett. 16 (1992) 231.
[60] D.S. Kim, I.E. Wachs, K. Segawa, J. Catal. 146 (1994) 268.
[61] J.A.R. Van Veen, H. De Wit, C.A. Emeis, P.A.J.M. Hendriks, J. Catal. 107 (1987) 579.
[62] H. Jeziorowski, H. Knozinger, J. Phys. Chem. 82 (1978) 2002.
[63] J.M. Stencel, L.E. Makovsky, T.A. Sarkys, J. De Vries, R. Thomas, J.A. Moulijn, J. Catal. 90 (1984) 314.
[64] A. Christodoulakis, E. Heracleous, A.A. Lemonidou, S. Boghosian, J. Catal. 242 (2006) 16.
[65] D. Nikolova, R. Edreva-Kardjieva, M. Giurginca, A. Meghea, J. Vakros, G.A. Voyiatzis, Ch. Kordulis, Vibr. Spectr. 44 (2007) 343.
[66] H. Jeziorowski, H. Knozinger, P. Grange, P. Gajardo, J. Phys. Chem. 84 (1980) 1825.
[67] L.H. Makovsky, J.M. Stencel, G.R. Brown, R.E. Tischer, S.S. Pollack, J. Catal. 89 (1984) 334.
[68] D. Nikolova, R. Edreva-Kardjieva, G. Gouliev, T. Grozeva, P. Tzvetkov, Appl. Catal. A: Gen. 297 (2006) 135.
[69] S. Rajagopal, H.J. Marini, J.A. Marzari, R. Miranda, J. Catal. 147 (1994) 417.
[70] A.J. Leonard, P. Ratnasamy, F.D. Declerck, J.J. Fripiat, Far. Disc. Chem. Soc. 54 (1971) 98.
[71] S. Rajagopal, J.A. Marzari, R. Miranda, J. Catal. 151 (1995) 192.
[72] J.A. Schwarz, B.G. Russell, H.F. Harnsberger, J. Catal. 54 (1978) 303.
[73] H.A. Benesi, B.H. Winquist, Adv. Catal. 27 (1978) 97.
[74] P. Arnoldy, M.C. Franken, B. Scheffer, J.A. Moulijn, J. Catal. 96 (1985) 381.
[75] P. Arnoldy, J.A. Moulijn, J. Catal. 93 (1985) 38.
[76] R. Lopez Cordero, F.J. Gil Llambias, A. Lopez Agudo, Appl. Catal. 74 (1991) 125.
[77] N. Spanos, A. Lycourghiotis, Langmuir 10 (1994) 2351.
[78] J.A. Bergwerff, T. Visser, B.M. Weckhuysen, Catal. Today 130 (2008) 117.
[79] M. Villarreal, P. Baeza, N. Escalona, J. Ojeda, B. Delmon, F.J. Gil-Llambıas, Appl. Catal. A: Gen. 345 (2008) 152–157.
[80] H. Topsøe, B.S. Clausen, F.E. Massoth, in: J.R. Anderson, M. Boudart (Eds.), Catalysis: Science and Technology, vol. 11, Springer-Verlag, Berlin, 1996.